

New Bending System Using a Segmented Vacuum Chuck for Stressed Mirror Polishing of Thin Mirrors

Pilseong Kang¹ and Ho-Soon Yang^{1,2*}

¹Advanced Instrumentation Institute, Korea Research Institute of Standards and Science, Daejeon 34113, Korea

²Department of Science of Measurement, University of Science & Technology, Daejeon 34113, Korea

(Received August 28, 2017 : revised October 23, 2017 : accepted October 23, 2017)

In the present research, a new bending system using a segmented vacuum chuck for Stressed Mirror Polishing (SMP) is developed. SMP is a special fabrication method for thin aspheric mirrors, where simple flat or spherical fabrication is applied while a mirror blank is deflected. Since a mirror blank is usually glued to a bending fixture in the conventional SMP process, there are drawbacks such as long curing time, inconvenience of mirror replacement, risk of mirror breakage, and stress concentration near the glued area. To resolve the drawbacks, a new bending system is designed to effectively hold a mirror blank by vacuum. For the developed bending system, the optimal bending load to achieve the designated mirror deflection is found by finite element analysis and an optimization algorithm. With the measurement results of the deflected mirror surfaces with the optimal bending loads, the feasibility of the developed bending system is investigated. As a result, it is shown that the bending system is appropriate for the SMP process.

Keywords : Aspheric mirror, Optical fabrication, Optimization, Stressed Mirror Polishing (SMP), Thin mirror
OCIS codes : (220.1080) Active or adaptive optics; (220.1250) Aspherics; (220.4610) Optical fabrication; (220.4880) Optomechanics

I. INTRODUCTION

Aspheric lenses and mirrors are designed to reduce aberration which frequently appears in a spherical lens or mirror. To remove the aberration, a multi-lens system is often used. However, a single aspheric lens can replace the much more complex multi-lens system. By using an aspheric lens or mirror, the overall optical system becomes simpler and lighter. In the past decades, the use of aspheric lenses and mirrors has been extended widely. The precision and efficiency of the fabrication and measuring techniques for aspherical optics, especially for large optics, have been improved by many researchers. Recently, large thin aspheric mirrors receive a lot of attention since they are necessary for the recently developed smart optical systems such as adaptive and active optical systems. Thus the fabrication and measuring techniques for large thin aspheric mirrors are matters of great interest.

Stressed Mirror Polishing (SMP), also called as Stress Mirror Polishing or Stress Polishing is one of the methods which can create large thin aspheric mirrors effectively. Since the origin of the method by Schmidt [1] in 1932, SMP has been developing continuously for high performance aspheric mirrors. The method is based on the theory of elasticity and the process is quite straightforward. First, a flat mirror blank is deflected to make the mirror surface be the inverse form of the desired aspheric surface. Then the deformed mirror surface is simply polished flat. After finish polishing, the applied load is removed and the polished surface springs back to the desired aspheric surface. Spherical polishing can be also used instead of flat polishing if the mirror blank is deflected as much as the gap between the desired aspheric surface and the spherical shape. SMP is applied iteratively until the peak to valley (PV) and root mean square (*rms*) surface error become less than 2 μm and 1 μm , respectively, for final

*Corresponding author: hsy@kriss.re.kr, ORCID 0000-0001-5699-8605

Color versions of one or more of the figures in this paper are available online.



This is an Open Access article distributed under the terms of the Creative Commons Attribution Non-Commercial License (<http://creativecommons.org/licenses/by-nc/4.0/>) which permits unrestricted non-commercial use, distribution, and reproduction in any medium, provided the original work is properly cited.

finishing such as ion beam figuring [9, 12, 17]. Although the application of this method is limited to relatively thin lenses or mirrors, there are various advantages. Since the classical flat or spherical polishing is used, the polishing process is quite simple. Also the removal rate is high because of polishing with a full size tool. Mid and high spatial frequency surface errors which frequently occur in the polishing with a small size tool can be reduced. In addition, mass producing of aspheric lenses or mirrors becomes possible since the same figure can be produced repeatedly with the same deflection.

There are various approaches for the bending of a mirror blank to make it the designated surface shape. The pioneering work of Schmidt [1] is well explained in the article by Everhart [2]. In the figuring of a Schmidt corrector plate which has an aspheric surface, the optical plate is spherically polished while it is deflected. The plate is supported by an O-ring gasket at its extreme boundary, and the deflection is made by a partial vacuum pressure applied to the lower side of the mirror. This method was improved by Lemaitre [3] in 1972. An oversized optical plate is supported on a narrow metal ring, and the vacuum pressure is applied partially to the bottom inner area. After finish of flat polishing, the desired aspheric optical surface is obtained by removing the load. With this approach, a more highly aspheric surface can be obtained conveniently. SMP has been applied to the fabrication of the Keck telescope's segmented mirrors. In the research by Lubliner and Nelson [4], they developed the theoretical basis of SMP to fabricate nonaxisymmetric mirrors for the Keck telescope's segmented mirrors. Also Nelson *et al.* [5] showed SMP as a technique for fabricating inexpensive high quality nonaxisymmetric mirrors and the convergence of the iterative spherical polishing. In this approach, a mirror blank is deformed prior to spherical grinding and polishing by applying a uniform pressure at the back side of the blank and applying shear forces and torques around its circumference. This approach is well explained in the literature of Mast and Nelson [6] also. Golden *et al.* [7] also investigated the practicality and economic feasibility of SMP for fabrication of large diameter off-axis segmented mirrors for Kitt Peak National Observatory. Hugot *et al.* [8] developed a manufacturing technique for a large thin glass shell of the deformable secondary mirror of the Very Large Telescope. In their technique, a thin mirror blank is placed on an aspheric mould with circular concentric holes and uniformly loaded by pressure, and then spherical grinding is applied. This method avoids unnecessary deformation of the thin mirror induced with a tool since the bottom of the mirror is supported by the mould instead of a single circular support ring. In the paper of Sporer [9], the feasibility of SMP for mirror segments of the Thirty Meter Telescope was investigated. In this research, a thin mirror is bonded with segmented annular pads of levers and loads are applied by actuators. The fabrication result of a full scale segment of the primary mirror is represented in

Daniel *et al.* [10]. It is shown that the required surface quality and the high material removal rates are obtained and the subsurface damage is low. By the research of Hugot *et al.* [11], the geometry of a mirror blank is optimized by finite element analysis (FEA) for the deformable secondary mirror of the Very Large Telescope. Laslandes *et al.* [12] performed research on SMP for the fabrication of the segmented mirrors of the European Extremely Large Telescope. An annulus warping harness is glued on the bottom of a circular mirror blank, and the bending forces are applied to the 12 arms connected to the harness. Research on improvement of SMP is still ongoing [13-19].

As mentioned above, SMP is a suitable and effective technique for fabrication of thin on- and off-axis aspheric mirrors. The designated deflection of a mirror blank is realized by different approaches, such as using vacuum and actuators. The attachment between a mirror blank and a fixture is usually made by gluing. In this case, curing time is needed and it is not convenient to change a mirror blank to another. Stress concentration near the glued area exists and there is a risk of mirror breakage when debonding.

In this paper, a new bending system using a segmented vacuum chuck is developed and built. With the new bending system, the inconvenience from bonding and debonding between a mirror blank and a fixture is removed. Thus, fast replacement of a mirror blank is possible in mass producing of aspheric mirrors. Before the design and instrumentation of an actuator-driven system as a future work, a manual bending system with a segmented vacuum chuck is designed and built for axisymmetric aspheric mirrors. The feasibility of the developed bending system and repeatability of mirror deflection are examined.

The outline of the paper is as follows. In Section 2, the process of stressed mirror polishing is briefly reviewed. Also, the developed bending system using a segmented vacuum chuck is described. Section 3 represents the optimization process of the bending load and the result. The measurement results of a mirror blank with applying the optimal bending loads in the bending system are represented in Section 4. The feasibility and repeatability are discussed. The paper is closed with conclusions in Section 5.

II. BENDING OF THIN MIRRORS IN STRESSED MIRROR POLISHING

2.1. Deflection of Mirror Blank

The brief description of SMP with flat fabrication is as shown in Fig. 1. A flat mirror blank is deformed as much as the inverse of the desired aspheric shape, then flat fabrication is performed to the mirror's top surface. After finish the fabrication, the load for mirror deflection is released and then the mirror surface becomes the desired aspheric surface. With this technique, complex aspheric fabrication is replaced by simple flat fabrication and spherical fabrication can be applied instead of flat fabrication.

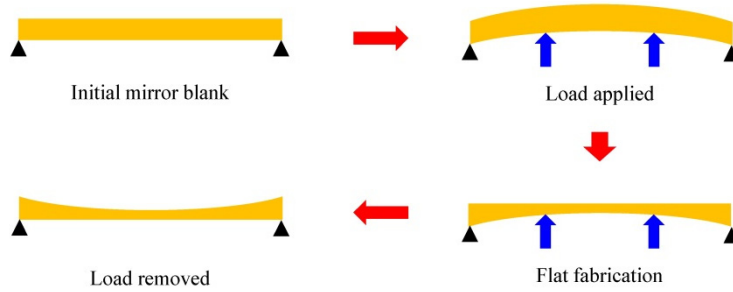


FIG. 1. Stressed Mirror Polishing (SMP) process with flat fabrication.

Since the SMP process is based on the elastic behavior of a mirror material, the accuracy of the fabricated mirror surface is based on the exactness of the mirror deflection. A concave aspheric optical surface is expressed by [20]

$$Z_a(r) = \frac{c_a r^2}{1 + \sqrt{1 - c_a^2 (1 + K) r^2}} + \sum_{i=2}^n A_{2i} r^{2i} \quad (1)$$

with the radius from the optic axis r , the inverse of the radius of curvature c_a , the conic constant K , and the coefficients of high order aspheric terms A_{2i} .

Also a concave spherical optical surface and a flat surface are defined as Eqs. (2) and (3), respectively.

$$Z_s(r) = \frac{c_s r^2}{1 + \sqrt{1 - c_s^2 r^2}} \quad (2)$$

with the radius from the optic axis r , the inverse of the radius of curvature c_s .

$$Z_f = 0 \quad (3)$$

Thus, the required deflection for spherical or flat fabrication in the SMP process is the difference between the desired aspheric surface and the spherical surface or between the desired aspheric surface and the flat surface. These are expressed as

$$Z_{def}(r) = Z_s(r) - Z_a(r) \text{ or } Z_{def}(r) = Z_f - Z_a(r) \quad (4)$$

If the bending load is applied by an annular support ring on a mirror blank, the deflection can be predicted by the theory of plates and shells by Timoshenko and Woinowsky-Kriger [21].

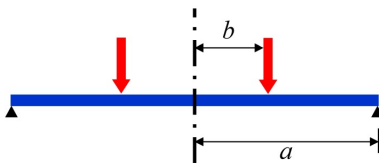


FIG. 2. A simply supported circular plate under concentric load.

For a circular plate simply supported at its boundary as shown in Fig. 2, the deflection w is described as Eq. (5) and (6) under a bending load F which is uniformly distributed along a circle of the radius b .

For $r \geq b$,

$$w = \frac{F}{8\pi D} \left[(a^2 - r^2) \left(1 + \frac{1}{2} \cdot \frac{1-\nu}{1+\nu} \cdot \frac{a^2 - b^2}{a^2} \right) + (b^2 + r^2) \log \frac{r}{a} \right] \quad (5)$$

For $r < b$,

$$w = \frac{F}{8\pi D} \left[(b^2 + r^2) \log \frac{b}{a} + (a^2 - b^2) \left(\frac{(3+\nu)a^2 - (1-\nu)r^2}{2(1+\nu)a^2} \right) \right] \quad (6)$$

where a is the outer radius of the circular plate, ν is the Poisson's ratio, and $D = Et^3 / 12(1 - \nu^2)$ is the rigidity of the plate with Young's modulus E and the plate thickness t .

The deflection with multi-bending loads can be predicted by using the method of superposition.

2.2. Mechanical Design of Bending System Using a Segmented Vacuum Chuck

In the present research, a new bending system with a segmented vacuum chuck is developed. The vacuum chuck is segmented into twelve pieces along its circumferential direction and each of them is designed to allow small tilting with a hinge. Thus, the deflected mirror surface can be smooth enough from the center to the boundary and the stress of the mirror blank can be reduced. Also fast and easy replacement of a mirror blank is possible by vacuum attraction.

The outline and the sectional view of the developed bending system with a segmented vacuum chuck are shown in Fig. 3. Figure 4 represents the developed bending system and the schematic of the vacuum system is as shown in Fig. 5.

A mirror blank is placed on the segmented vacuum chuck and the bending load is applied by lifting a support ring under the mirror blank with a precise lab-jack. The

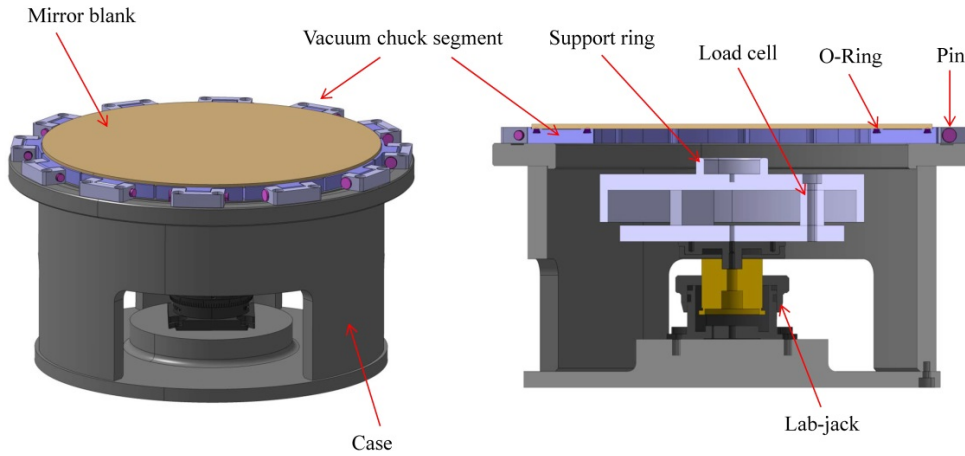


FIG. 3. 3D model of the bending system and its sectional view.

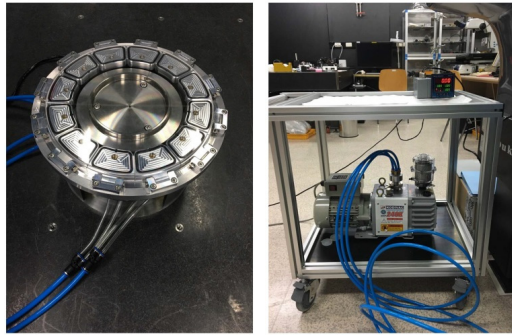


FIG. 4. The developed bending system using a segmented vacuum chuck.

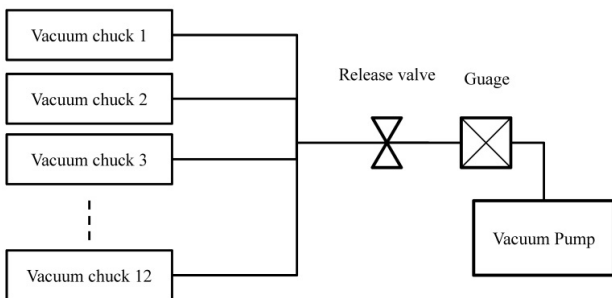


FIG. 5. Schematic of vacuum system.

applied load value is measured by three load cells positioned between the support ring and the lab-jack, and the summed load is displayed on an indicator. A mirror blank and a vacuum chuck segment are sealed with O-ring and the applied vacuum pressure between them is -0.95 bar.

III. OPTIMIZATION OF BENDING LOAD

3.1. Optimization Process of Bending Load

To increase the accuracy of the amount of mirror deflection, the optimal bending load to make the designated

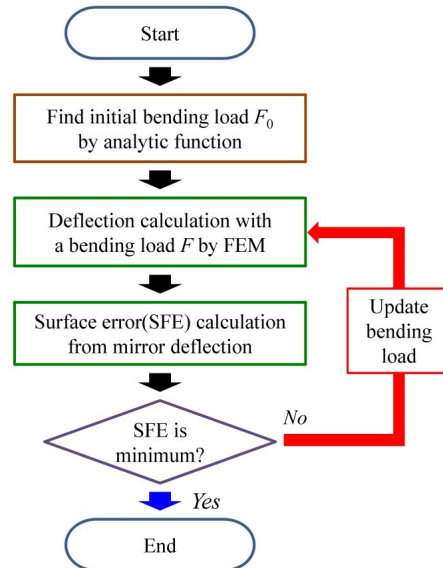


FIG. 6. Flow chart of bending load optimization.

deflection of a thin mirror blank for flat fabrication should be found. Even though the bending load F can be found analytically with Eqs. (5) and (6), the derived bending load from these equations could not make the designated deflection of the mirror blank exactly in the physical bending system since the complex geometry and boundary conditions are not reflected on the analytic formulas. Thus, the deflection of a mirror blank in the bending system is analyzed by finite element analysis (FEA), and the required bending load to obtain minimum surface error between the deflected surface and the designated aspheric surface is found by an optimization algorithm with the result of FEA. This process is described in Fig. 6.

The optimization problem is stated as Eq. (7). The design variable is the bending load F applied to the support ring and the objective function is *rms* surface error between the deflected surface by the bending load and the designated aspheric surface.

$$\begin{aligned}
 &\text{Find bending load } F \\
 &\text{minimize } rms \text{ surface error} \\
 &\text{subject to } F_{low} \leq F \leq F_{upp}
 \end{aligned} \tag{7}$$

The bending load F found by Eqs. (5) and (6) is set as the initial value of the design variable F for the optimization using FEA. Once the deflection of a mirror blank is analyzed by FEA with a bending load, the objective function, rms surface error, is calculated from the displacement of the mirror surface. The bending load is continuously updated until the rms surface error is minimized.

The FEA is performed using the commercial design and simulation software CATIA and the optimization process is coded by Matlab. A function $fmincon$ is used as the optimization algorithm, and CATIA and Matlab are connected via a CATIA macro file.

3.2. Optimization Result of Bending Load

Maximum sag and maximum aspect ratio of the target aspheric mirror depend on the strength limit of the mirror material. These should be set to be safe from mirror breakage by bending. In practical application of the Thirty

TABLE 1. Specification of the target aspheric mirror

| | |
|---------------------|-----------|
| Material | Quartz |
| Diameter | 250 mm |
| Thickness | 3 mm |
| Clear aperture | 160 mm |
| Radius of curvature | 20,000 mm |
| Conic constant (K) | -1.000953 |
| Maximum sag | 0.25 mm |

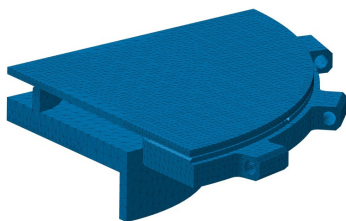


FIG. 7. Finite element model of the quarter model with $\Phi 40$ mm support ring.

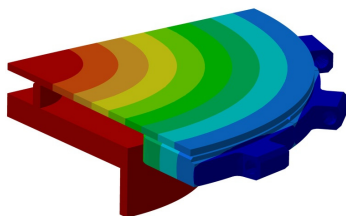


FIG. 8. Analysis result of the quarter model with $\Phi 40$ mm support ring.

Meter Telescope (TMT), the diameter of a mirror is 1200 mm and the thickness is 40 mm with Zerodur. The aspect ratio is 30:1 and the sag is 3 mm [9]. Since the developed bending system in the present paper is a prototype for a 250 mm diameter mirror, the aspect ratio and the sag are set conservatively. However, the values are set enough for checking the feasibility. The specification of the target aspheric surface is as listed in Table 1.

For flat fabrication, the required bending load is optimized with respect to three different radii support rings with the analytic formulas and FEA. In FEA, the unnecessary parts of the bending system are omitted and a quarter of the bending system is considered due to the axisymmetry. Figure 7 shows the finite element model and the total number of nodes is 246,579 and the number of elements is 167,828. The materials of the vacuum chuck and the support ring are Al6061 and SUS303, respectively. The symmetric boundary conditions are applied at the x-z plane and y-z plane of the quarter model and the contact condition is applied between the mirror blank and the support ring.

Figure 8 represents an example of analysis result when $\Phi 40$ mm support ring is used, and Fig. 9 shows the

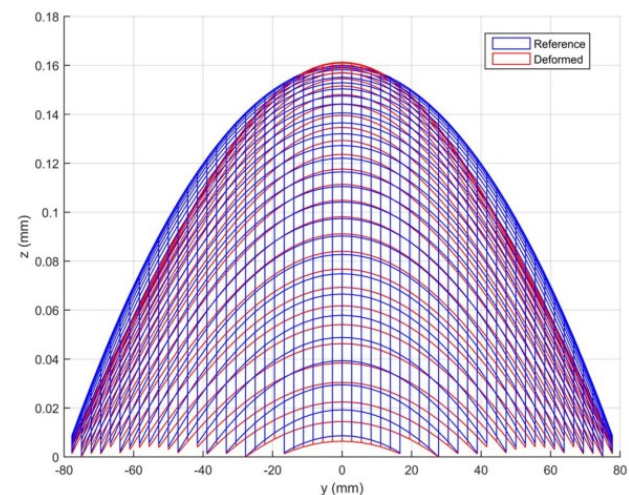
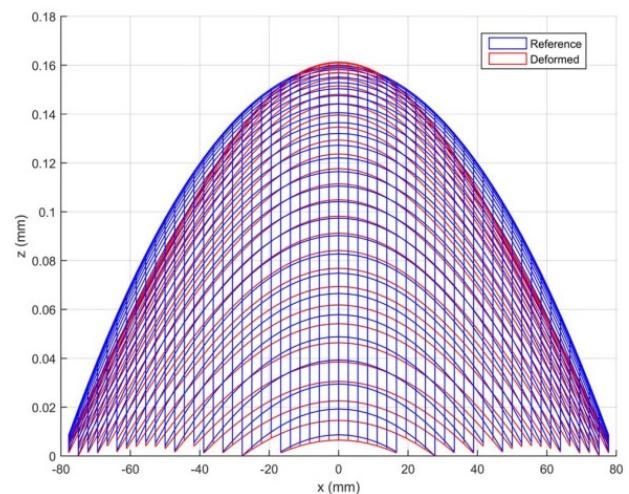


FIG. 9. Deformed mirror surface with $\Phi 40$ mm support ring.

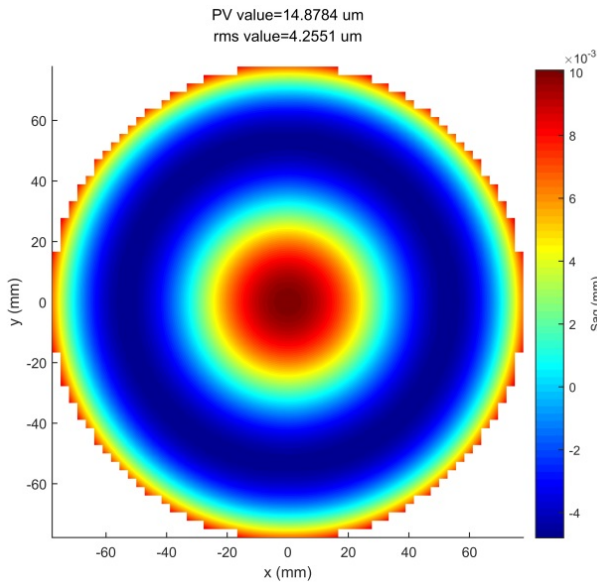


FIG. 10. Surface error contour with $\Phi 40$ mm support ring.

deformed mirror surface compared with the designated aspheric surface. By using the displacement of mirror surface extracted from the FEA result, *rms* surface error is calculated and the result is shown in Fig. 10.

Figure 11 represents the optimization result with $\Phi 40$ mm support ring by the process described in Fig. 6. Figure 11(a) and 11(b) are the convergence of the normalized objective function and the convergence of the normalized design variable, respectively. As mentioned above, the design variable is the bending load applied to the support ring, and the objective function is the surface error between the deflected surface by a bending load and the required deflection calculated by Eq. (4). It can be seen that they are converged properly in 35 iterations. The surface error

TABLE 2. Optimization result

| Ring size (diameter) | 40 mm | 80 mm | 120 mm |
|------------------------------|---------------------|--------------------|--------------------|
| Optimal bending load | 79.4 N | 97.0 N | 134.3 N |
| Surface error (<i>rms</i>) | 4.27 μm | 2.05 μm | 0.33 μm |
| Surface error (PV) | 14.91 μm | 7.61 μm | 1.68 μm |

is minimized with the optimal bending load at iteration 35, which means that the mirror blank can be set for flat fabrication with the optimal bending load.

The optimizations of the bending load for $\Phi 80$ mm and $\Phi 120$ mm support rings are also performed. Table 2 shows the optimization results with respect to the support ring sizes. It can be seen that the *rms* surface error is smaller with larger ring size and the surface error is low enough for SMP.

IV. VALIDATION OF MIRROR DEFLECTION

4.1. Measurement of Deflected Mirror Surface

The optimal bending load with respect to the support ring size is applied to the mirror blank in the developed bending system. The deflected mirror surface is measured by a Coordinate Measuring Machine (CMM) and the results are compared with the simulation results.

Figure 12 show the surface error contours with respect to the support ring sizes.

The *rms* surface error values of the support rings $\Phi 40$ mm, $\Phi 80$ mm, and $\Phi 120$ mm are 5.2 μm , 3.2 μm , and 2.5 μm , respectively. To check whether the obtained *rms* surface error is minimum or not, the additional measurements are performed at ± 5 N from the optimal bending load values. Figure 13 represents the variations of the *rms* and PV surface errors with respect to the support ring sizes.

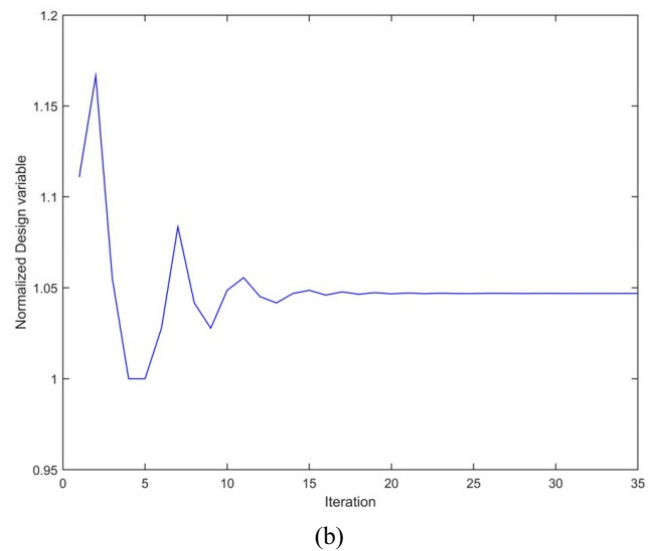
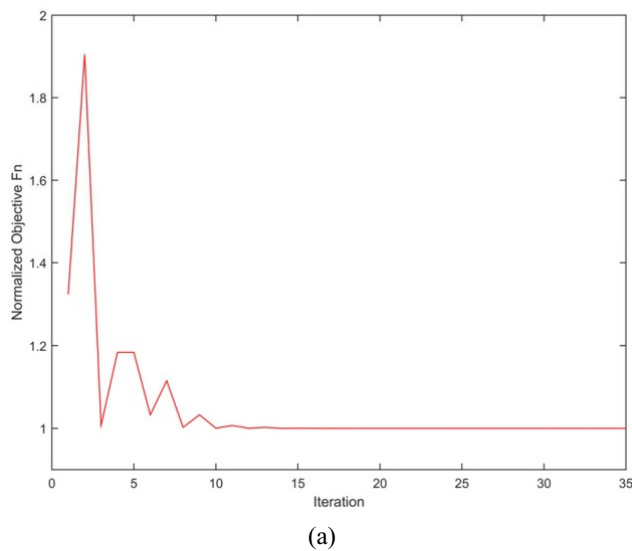


FIG. 11. Optimization result with $\Phi 40$ mm support ring: (a) convergence of normalized objective function; (b) convergence of normalized design variable.

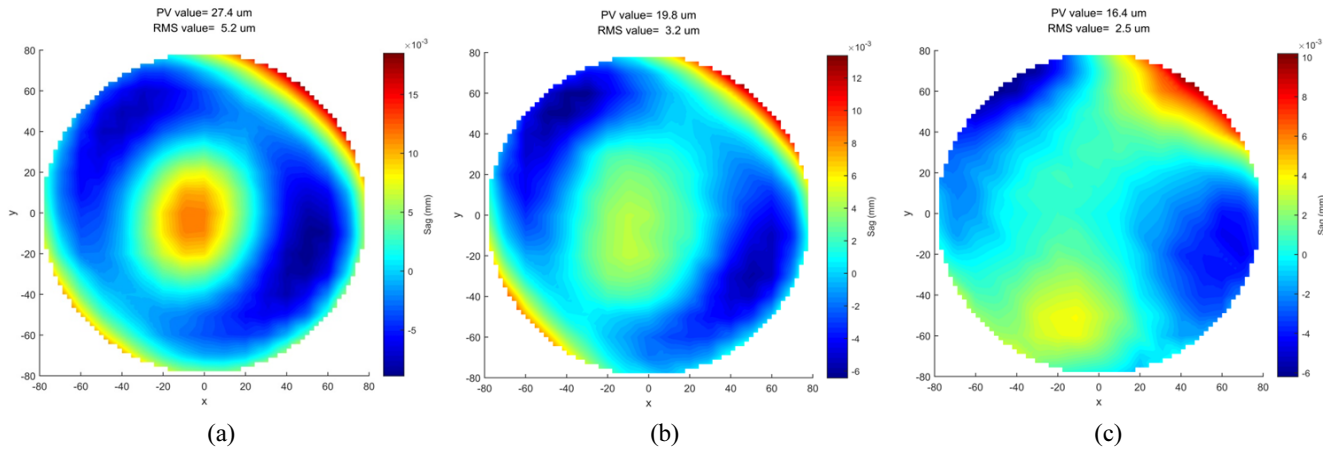


FIG. 12. Surface error contour (a) with $\Phi 40$ mm support ring, (b) with $\Phi 80$ mm support ring, (c) with $\Phi 120$ mm support ring.

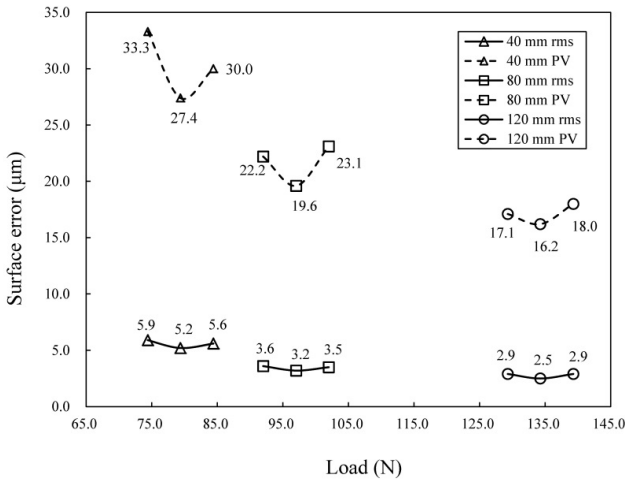


FIG. 13. Surface error variation with respect to support ring size.

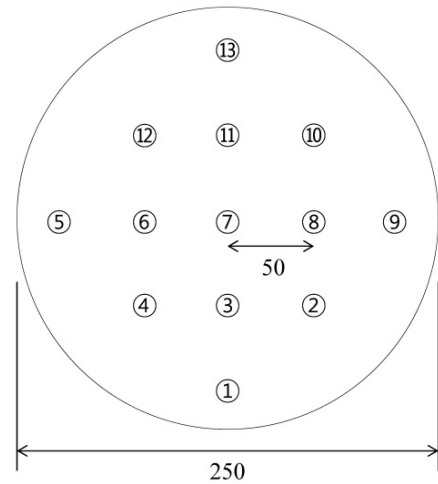


FIG. 14. Measurement points for validation of repeatability.

It is shown that the *rms* and PV surface errors at the optimal bending loads are lowest values and the optimization with FEA is well performed for predicting the required bending load. Compared to the results with the simulation results, there are differences on *rms* and PV values, but the differences are small and the tendency is to be very close to each other. In addition, the surface errors could be reached to the target values since iterative SMP is generally performed.

4.2. Repeatability of Mirror Deflection

For mass producing of thin aspheric mirrors by SMP, repeatability of generating the aspheric surface shape should be established. To validate the repeatability in the developed bending system, the deformed mirror surface with $\Phi 40$ mm support ring in 90 N bending load is measured five times and the results are compared. For each measurement, the mirror is replaced and the vacuum pressure is reset, then the same bending load is applied again. Figure 14 represents the measuring points and the result is shown in Fig. 15

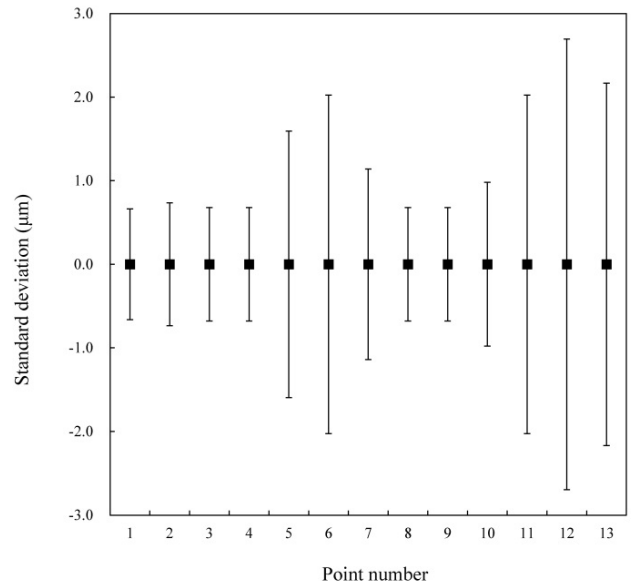


FIG. 15. Repeatability test result at measurement points.

where each error bar means the standard deviation from the average of each measuring point. As a result, the standard deviations are around 2 μm and the maximum value is less than 3 μm . Considering the measurement uncertainty of the CMM which is 2.2 μm (95% confidence level, $k=2$), it can be seen that the bending system shows appropriate repeatability.

V. CONCLUSION

In the present research, a new bending system using a segmented vacuum chuck for SMP is developed and tested. The bending load to achieve the designated aspheric surface for flat fabrication in the process of SMP is optimized via FEA and an optimization algorithm. Then a mirror blank is deflected with the optimized bending load, and the measurement result of the deflected surface is compared with the designated aspheric surface. It is shown that the developed bending system can realize the required deflection of a mirror blank properly, and the repeatability of mirror deflection is also validated. The drawbacks coming from the gluing are removed by the bending system, and it is expected that the time and cost for preparing of an aspheric mirror before the final finishing can be reduced. As a future work, an actuator-driven bending system will be built with a segmented vacuum chuck for compensating local surface errors. With a segmented support with a number of actuators, the generation of mirror deflection for a nonaxisymmetric aspheric surface can be achieved. Also, the fabrication of nonaxisymmetric aspheric mirrors will be successfully converged with iterative deflections by controlling the actuators. Although the optimal bending loads are found by the optimization algorithm and FEA in the present research, the real time wavefront sensing by an interferometer or a deflectometry technique would be very helpful to find the optimal bending loads in the future work.

REFERENCES

1. B. Schmidt, "A coma free telescope," *Mitt. Hamb. Strenv.* **7**, 15 (1932).
2. E. Everhart, "Making corrector plates by Schmidt's vacuum method," *Appl. Opt.* **5**(9), 1360 (1966).
3. G. Lemaitre, "New procedure for making schmidt corrector plates," *Appl. Opt.* **11**(7), 1630-1636 (1972).
4. J. Lubliner and J. E. Nelson, "Stressed mirror polishing. 1: A technique for producing nonaxisymmetric mirrors," *Appl. Opt.* **19**(14), 2332-2340 (1980).
5. J. E. Nelson, G. Gabor, L. K. Hunt, J. Lubliner, and T. S. Mast, "Stressed mirror polishing. 2: Fabrication of an off-axis section of a paraboloid," *Appl. Opt.* **19**(14), 2341-2352 (1980).
6. T. S. Mast and J. E. Nelson, "The fabrication of large optical surfaces using a combination of polishing and mirror bending," *Proc. SPIE* **1236**, 670-681 (1990).
7. L. Golden, P. Gillett, R. Radau, J. Richardson, and G. Poczulp, "Stressed mirror polishing experiment underway at kitt-peak-national-observatory," *Proc. SPIE* **0332**, 357-365 (1982).
8. E. Hugot, M. Ferrari, D. Fappani, and R. Arsenault, "Active polishing of a 2 mm thin shell for large adaptive secondary mirrors," *Proc. SPIE* **6272**, 62724Z (2006).
9. S. F. Sporer, "TMT: stressed mirror polishing fixture study," *Proc. SPIE* **6267**, 62672R (2006).
10. J. Daniel, U. Mueller, T. Peters, S. F. Sporer, and T. Hull, "Tinsley progress on stress mirror polishing (SMP) for the Thirty Meter Telescope (TMT) primary mirror segments II," *Proc. SPIE* **7733**, 773328 (2010).
11. E. Hugot, M. Ferrari, A. Riccardi, M. Kompero, G. R. Lemaitre, R. Arsenault, and N. Hubin, "Stress polishing of thin shells for adaptive secondary mirrors," *Astron. Astrophys.* **527**, A4 (2011).
12. M. Laslandes, N. Rousselet, M. Ferrari, E. Hugot, J. Floriot, S. Vivès, G. Lemaitre, J. F. Carré, and M. Cayrel, "Stress polishing of E-ELT segment at LAM: full-scale demonstrator status," *Proc. SPIE* **8169**, 816903 (2011).
13. X. Li, Z. Jiang, X. Gong, H. Zhang, K. Chen, Y. Zheng, B. Li, B. Yu, C. Xu, B. Ji, and Q. Xu, "Stressed mirror annular polishing for scale-down TMT primary segments," *Proc. SPIE* **9912**, 99120A (2016).
14. C. Li, B. Lei, and Y. Han, "The advancement of the high precision stress polishing," *Proc. SPIE* **9683**, 96831F (2016).
15. J. Z. Bo, L. X. Nan, Y. B. Bin, Z. Yi, and L. Bo, "Influence and control of spherical aberration in polishing off-axis aspherical mirrors by the stressed method," *Appl. Opt.* **54**(2), 291-298 (2015).
16. Y. Han and L. Lu, "Stressed mirror polishing: finite element simulation of mirror blank deformation," *Proc. SPIE* **9281**, 92810W (2014).
17. E. Hugot, A. Bernard, M. Laslandes, J. Floriot, T. Dufour, D. Fappani, J. M. Combes, and M. Ferrari, "Stress polishing demonstrator for ELT M1 segments and industrialization," *Proc. SPIE* **9145**, 914539 (2014).
18. R. Izazaga-Pérez, D. Aguirre-Aguirre, F. Granados-Agustín, and M. Percino-Zacarias, "Optical testing and finite element analysis applied in stressed mirror polishing," *Proc. OSA, OM3C.6* (2014).
19. L. Xin-nan, Z. Hai-ying, C. Xiang-qun, J. Zi-bo, Z. Yi, L. Xing-tao, and N. Hou-kun, "Study on the stressed mirror polishing with a continuous polishing machine for large aperture off-axis aspheric mirrors," *Chin. Astron. Astrophys.* **36**(4), 435-444 (2012).
20. C. Pruss, E. Garbusi, and W. Osten, "Testing aspheres," *Opt. Photon. News* **19**(4), 24-29 (2008).
21. S. P. Timoshenko and S. Woinowsky-Krieger, *THEORY OF PLATES AND SHELLS* (McGraw-Hill, 1959).